CHEMISTRY
A EUROPEAN JOURNAL

DOI: 10.1002/chem.201204242

Elusive Nanoscale Metal–Organic-Particle-Supported Metallogel Formation Using a Nonconventional Chelating Pyridine–Pyrazole-Based Bis-Amide Ligand

Satirtha Sengupta* and Raju Mondal*[a]

Dedicated to Professor Judith A. K. Howard, CBE, FRS

Nanoscale metal–organic particles (NMOPs) have recently gained immense importance as hybrid materials because they show promising applications in various fields including drug delivery, chemo- and biosensing, molecular electronics, and as contrast agents in magnetic resonance imaging.[1] One of the most interesting and useful features of NMOPs is their ability to entrap guest molecules that range from drug molecules[1b,e] to greenhouse gases and organic dyes.[2] Notwithstanding these successes, entrapment of solvent molecules by using NMOPs for metallogel formation is extremely rare.[3] It is worth mentioning here that the self-assembly process in the run up to the gel formation usually takes place unidimensionally to generate a fibrous morphology. Metallogels, a fast-expanding branch of supramolecular gels, are formed when a discrete metal complex self-assembles by means of noncovalent interactions to give rise to a highly cross-linked, intertwined, three-dimensional network while immobilizing a large amount of solvent molecules within the framework. With the proper choice of the gelators and transition metals, metallogels can be successfully tuned to impart physicochemical properties such as magnetic, spectroscopic, and catalytic properties.[4] Introduction of functional groups such as urea, amide, and aromatic rings, which are capable of forming various weak interactions like hydrogen bonding or π–π stacking, have been found to be instrumental in immobilizing solvent molecules. On the other hand, ligands with multiple coordinating sites were found to promote the requisite cross-linking network.[5]

However, even a cursory inspection would reveal that most of the strategies adopted for generating metallogels are more or less “one-dimensional”, that is, they use a divergent *exo*-ditopic ligand with a single coordinating site, with an overwhelming majority of urea- and amide-based bipyridyl molecules.[5,6] In principle, as far as gel formation is concerned, one can argue that there is a serious shortcoming in pyridine-based bis-urea or bis-amide complexes. These types of divergent bipyridine-based ligands have a natural tendency to form solid polymeric coordination polymers or MOFs, which goes against the basic principle of gel formation. Considering the fact that gel formation represents a tradeoff between the dynamic solution phase and solid aggregate, any judicious design of gelator molecule should aim to restrict coordination polymer formation. Therefore, a convergent chelating ligand should always have an edge over a divergent ligand, provided the former type is still capable of immobilizing large amount of solvents. The sheer dominance of bent 3-pyridyl-based ligands over the linear 4-pyridyl-based ligands in gel formation can be envisaged as corroborating evidence for this theory.

Inspired by the above-mentioned considerations, we have successfully evaluated the usefulness of chelating ligands in metallogel formation by using a simple pyridine–pyrazole-based ligand, N^1,N^3-bis[5-(pyridin-2-yl)-1*H*-pyrazole-3-yl]-isophthalamide (BPPIPA). To the best of our knowledge, this is the first example in which a bis-amide-based chelating ligand has been used for metallogel formation. We chose a pyridine–pyrazole moiety for two reasons: 1) pyrazole-based compounds are biologically important molecules owing to their antibacterial, antifungal, and antimicrobial properties;[7] and 2) the pyrazole group can play a dual role in metal coordination as well as hydrogen-bond formation with solvents using the built-in hydrogen-bonding site (N–H).

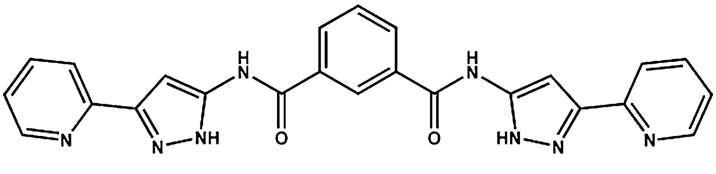

BPPIPA

BPPIPA can be prepared in high yields by the reaction of 3{5}-amino-5{3}-(pyrid-2-yl)-1*H*-pyrazole[8] with isophthalolyl chloride in the presence of triethylamine. BPPIPA itself is

---

[a] S. Sengupta, Dr. R. Mondal
Department of Inorganic Chemistry
Indian Association for the Cultivation of Science
2A & 2B Raja S.C. Mullick Road
Kolkata 32, W.B. (India)
Fax: (+91) 33-2473-2805
E-mail: icrm@iacs.res.in

Supporting information for this article is available on the WWW under http://dx.doi.org/10.1002/chem.201204242. It contains a picture of the metallogels, elemental analysis, plots of the elastic modulus of copper bromide gel, SAED diffraction patterns, FTIR spectra, EDAX spectra, powder diffraction patterns of the xerogels, and the local structure of the gel.

not a gelator, but in the presence of copper chloride and bromide it gives rise to a green transparent gel instantaneously. The ligand is soluble in a wide variety of solvents such as hot THF, 1,4-dioxane, DMF, and DMSO. It can gel copper halides in all the aforementioned solvents in the presence of water as cosolvent, but gel formed in DMF/water (3:2) was found to be the strongest amongst all and hence is discussed in detail in this Communication. Addition of copper halide (0.1 to 0.4 equiv with respect to the ligand concentration) to a 1 wt% ligand solution (critical gel concentration) in a DMF/water mixture gave partial gels, but the addition of copper salt (0.5 equiv) instantly gelled the total mixture. Complete gels were obtained up to 1.0 equiv copper halide concentration, after which partial gels were formed (see Figure S1 in the Supporting Information). The ligand is highly selective towards copper halides because no gels formed with other copper analogues and other first-row transition metals under similar conditions. A sample of freshly prepared gel without sonication exhibited thixotropic behavior by transforming into a viscous sol upon shaking, which re-formed into gel upon standing. Moreover, the gel that re-formed was found to be stronger than the gel obtained initially. However, stronger gels can also be obtained by brief sonication of the freshly formed gel. Polar solvents, especially water, were found to be imperative towards gelation as no gels were formed in nonpolar solvents . The sol–gel transition temperature, T_{gel}, as determined by the dropping-ball method was found to be (65 ± 3) °C for 0.5 equiv copper chloride, which increased to (80 ± 3) °C for 0.6 equiv copper chloride, above which the gel persisted beyond the boiling point of water suggesting high thermal stability of the gels. However, the T_{gel} value for copper bromide gel was found to be slightly higher than its chloride counterpart with (70 ± 3) °C for 0.5 equiv copper bromide, which increased to (83 ± 3) °C for 0.6 equiv copper bromide. Wherever observed, the gels were thermoreversible and stable under ambient conditions on a bench top over several weeks.

Elemental analysis (see Table 1 in the Supporting Information) performed with the xerogels revealed a 1:1 stoichiometry of ligand/metal irrespective of the copper concentrations.

To probe the participation of the amide groups in the self-assembly process through hydrogen-bonding interactions, infrared spectroscopy was performed with the free ligand and its corresponding xerogel (see Figure S6 in the Supporting Information). The ligand displayed strong absorption bands at 3454, 1674, and 1541 cm^{-1} that correspond to N–H stretching, C=O stretching vibrations, and N–H bending vibrations of the amide groups, respectively, which shifted to 3413, 1608, and 1546 cm^{-1} in the copper chloride xerogel. The decrease in the N–H and C=O stretching frequency in the xerogel coupled with an increase in the N–H bending vibration band supports the fact that significant intermolecular hydrogen bonding between the carbonyl oxygen atom and the amide hydrogen atom has taken place in the gel state. Moreover, the stretching vibrations of C=N bonds in pyrazole and pyridine groups at 1495 and 1579 cm^{-1}, respectively, in the ligand shifted to 1467 and 1570 cm^{-1} in the xerogel, thereby suggesting metal coordination to both the pyridine and pyrazole nitrogen. Copper bromide gel exhibited similar behavior with the N–H stretching, C=O stretching, and N–H bending of the amide functionality shifting to 3411, 1604, and 1544 cm^{-1}, respectively, in the xerogel, whereas the C=N stretching of pyrazole and pyridine was observed at 1469 and 1571 cm^{-1}, respectively.

To gain insight into the absorption properties of the ligand and its metal complexes, UV/Vis titration (Figure 1) was carried out by taking a 1×10^{-5} M concentration (in 3:2 DMF/water mixture) of the ligand and sequentially adding measured aliquots of metal salt solution into it. A strong π–π^* absorption band appeared at 285 nm in the free ligand, which redshifted to 292 nm upon sequential addition of metal salt solution up to 2 equiv of copper, with the peak

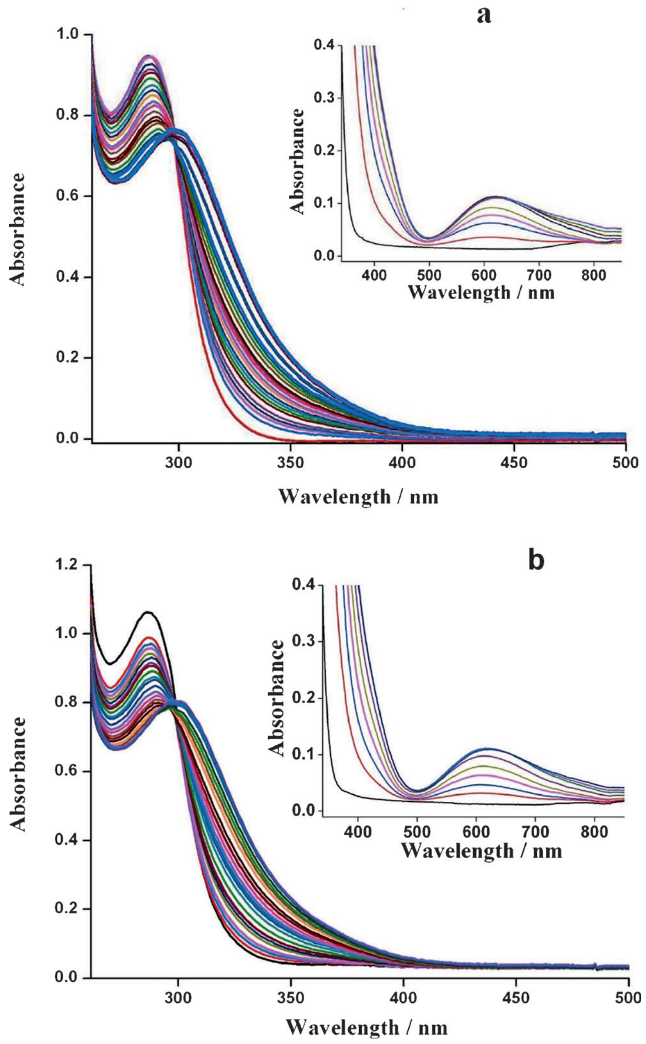

Figure 1. UV/Vis absorption spectra of ligand titrated with a) aliquots of copper chloride (runs of 0.1 up to 2 equiv, 0.2 up to 4 equiv), and b) aliquots of copper bromide (runs of 0.1 up to 2 equiv, 0.2 up to 4 equiv). Inset images show the corresponding d–d transitions.

gradually decreasing in intensity. A weak, broad band at around 320 nm in the free ligand spectrum, which might be attributed to intraligand charge transfer (ILCT), showed a gradual increase in energy without any significant shifting of the peak. However, a further increase in the copper salt concentration from 2 to 4 equiv resulted in the generation of separate absorption peaks at around 300 nm without any significant change or shift, which suggests complete complexation of the metal with the ligand at 2 equiv of copper, above which the spectra of the copper–ligand complex was observed. Moreover, increasing the concentration of the ligand to 10^{-3} M and subsequently titrating with aliquots of the corresponding copper salts gave a broad peak (due to ligand field and Jahn–Teller effects) centered around 600–650 nm (Figure 1, inset), which corresponded to a d–d (${}^2E_g \rightarrow {}^2T_{2g}$) transition, thus indicating octahedral geometry around the metal ion.

Furthermore, EPR spectroscopy was used as a tool to determine the environment around the copper ion, which showed a similar spectrum both for the copper chloride and its bromide analogue at all copper concentrations. The X-band ESR spectrum (see Figure S5 in the Supporting Information) recorded at 77 K revealed anisotropic character that contained four poorly resolved super hyperfine absorption-like peaks that correspond to $g_{||}$, thus indicating the interaction of the copper(II) odd electron with four similar atoms, which in the present case is nitrogen. Moreover, the g-tensor values, $g_{\|}(2.34) > g_{\perp}(2.04) > 2.0023$, indicate that the ground state of copper is predominantly $d_{x^2-y^2}$ and has a distorted-octahedral geometry with axial symmetry. The exchange interaction parameter G value (calculated as $G = (g_{\|}-2)/(g_{\perp}-2)$) was found to be 8.5 (that is, $G > 4$), which indicates that the exchange interaction between copper centers in the gel state is negligible. Moreover, the absence of any half-field signal around 1600 G due to a $\Delta M_s = \pm 2$ transition also rules out any Cu–Cu interaction, which suggests that the complex is mononuclear. Thus, on the basis of the above spectral studies and elemental analysis taken together, we can propose that the copper atom forms a distorted-octahedral geometry with four nitrogen atoms of two chelating BPPIPA molecules occupying the equatorial position, whereas the axial positions are occupied by chlorine atoms. This gives rise to a one-dimensional infinite network, which can be considered the basic building unit of gel. Subsequently, higher dimensionality is achieved through hydrogen bonding and π–π stacking among these one-dimensional strands, as shown in Figure S8 in the Supporting Information.

The strength of the copper halide gels of BPPIPA (1 wt %) was further probed by using stress sweep rheometry (Figure 2) in which the viscous modulus and the elastic modulus was measured as a function of increasing strain amplitude from 0.01 to 200 % keeping the frequency constant at 1 Hz and temperature at 298 K. In both cases, the viscous modulus (G'') was found to be less than the elastic modulus (G'), which is suggestive of gel-like materials by one order of magnitude. Both the values of G' and G'' were found to be nearly constant up to about 6 % strain, which denotes the linear viscoelastic region (LVR), after which a steep drop in the values of both the moduli was observed, thereby suggesting complete disruption of the gel network. The strength of copper bromide gel was found to be slightly greater than that of its chloride analogue, which in turn was strongly dependent on the concentration of copper added, with the strength gradually increasing up to 0.8 equiv of copper halides, after which it decreased. However, even the strongest gel at 0.8 equiv of copper displayed an elastic modulus of about 1200 Pa with a yield stress of about 85 Pa, which suggests the formation of a moderately strong metallogel.

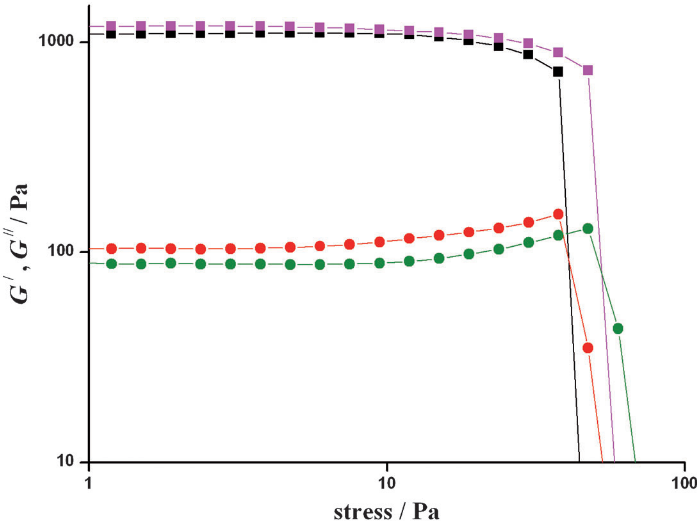

Figure 2. Plot of elastic modulus (G', black squares) and viscous modulus (G'', red circles) for copper bromide gel, and elastic modulus (G', magenta squares) and viscous modulus (G'', green circles) for copper chloride gel as a function of applied stress [Pa] for 1 wt % gel prepared by using 0.8 equivalents of copper halide.

Furthermore, to study the morphology of the metallogel, field-emission scanning electron microscopy (FESEM) and transmission electron microscopy (TEM) were performed on the xerogels. A freshly prepared sample of the xerogel revealed an aggregation of numerous spherical particles (NMOPs) of an approximate diameter that ranged from 50 to 120 nm (Figure 3a, b), which was also visible even in the sol state (Figure 3c), but with a considerable decrease in size. The gel that re-formed from the sol state as well as the gel that formed after sonication was found to contain slightly larger NMOPs with an average diameter of 200 nm (Figure 3d). Since these NMOPs are smaller in size they are supposed to provide a large surface area that could support many interparticle cross-linking sites in the network, which can effectively interact with and entrap the solvent molecules that can give rise to the increased stability of the gel in a polar aqueous solvent medium.[3] However, over a course of several weeks, these particles underwent a morphological transformation to a fibrillar structure (Figure 3e), even though very small NMOPs were still visible in the TEM micrograph. Moreover, the formation of these NMOPs was further confirmed by using atomic force microscopy (AFM)

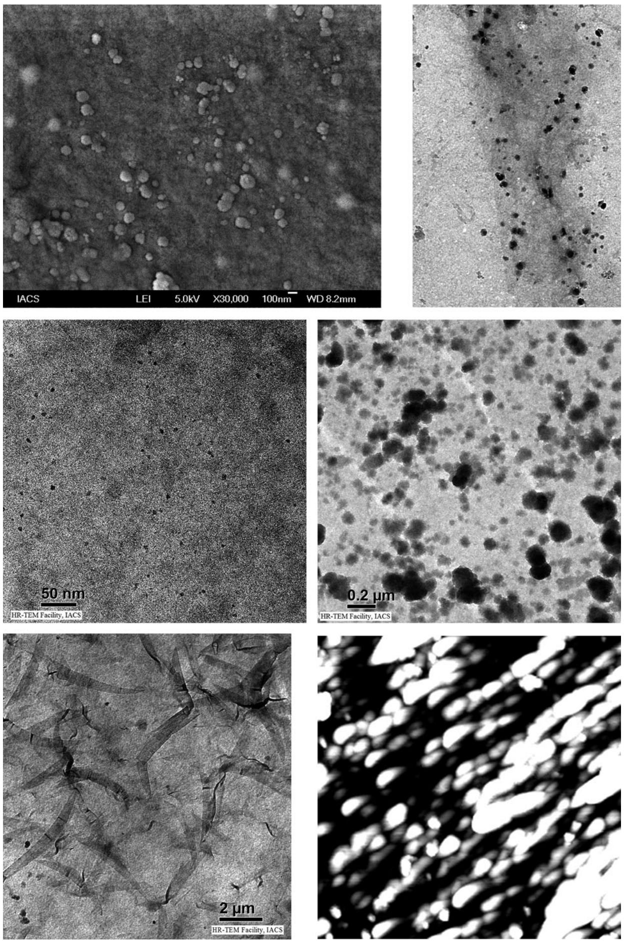

Figure 3. a) SEM image of NMOPs. TEM images of b) freshly prepared copper chloride gel, c) sol after shaking, d) gel after sonication, e) NMOPs transformed to fibers after about a month. f) AFM images of NMOPs (note that the spherical particles are highly deformed, which might be due to the expulsion of solvent molecules while drying).

(Figure 3f). AFM performed on xerogels revealed that the NMOPs had a base size that varied from 100 to 200 nm with heights that ranged from 40 to 100 nm. Nevertheless, the spheres were highly deformed, which might be due to the exudation of solvent molecules while drying. To the best of our knowledge, this is the first report of NMOPs that support metallogel formation by using a pyridine–pyrazole-based bis-amide molecule.

Selected-area electron diffraction (SAED) performed on these NMOPs revealed the individual particles to be crystalline in the case of copper chloride gel but amorphous in the case of copper bromide gel (see Figure S3 in the Supporting Information). This is attributed to the fact that crystals begin to grow within the copper chloride gel matrix over a period of a few weeks, the microcrystalline nature of which prevented their crystal structure determination. However, no such phenomenon was observed in its bromide analogue, thereby accentuating the fact that the initial NMOPs that constituted the copper chloride gel crystallized within the gel matrix over a month, although no direct evidence of it could be obtained. Energy-dispersive X-ray spectroscopy (EDAX) analysis performed on these NMOPs (Figure S4 in the Supporting Information) was found to contain both the ligand and the metal elements, which ruled out the possibility of generation of copper nanoparticles within the gel matrix. Moreover, this microcrystallization is supported by the powder XRD pattern of the xerogels (Figure S6 in the Supporting Information), which revealed the slightly crystalline nature of the copper chloride gel, but its bromide analogue was completely amorphous.

In conclusion, we have reported for the first time, to the best of our knowledge, a novel pyridine–pyrazole-based bis-amide molecule that is capable of chelating copper chloride and bromide to form instantaneously green transparent gels. Primary investigation revealed the gels to be made up of recently discovered nanoscale metal–organic particles (NMOPs), which find useful applications in the field of medicine and nanotechnology. Fresh gels were found to be mechanoresponsive to stress and displayed pronounced thixotropic behavior. However, sonication leads to the formation of stronger gels having high thermal stability. The ligand was found to be highly selective toward copper halides only, thus making it a good candidate for both selective cation and anion capture. Further studies on gelation with the pyridyl–pyrazole amine in the generation of other aromatic and aliphatic amides are being pursued in our lab.

Acknowledgements

R.M. gratefully acknowledges financial assistance from the Council of Scientific and Industrial Research (CSIR), India (01(2327)/09/EMR II/CSIR). S.S.G. is thankful to CSIR, India for research fellowships. S.S.G. also acknowledges Anindita Das, Polymer Science Unit, for helping in rheology experiments and Debajyoti Pramanik, Department of Inorganic Chemistry, for assisting in UV/Vis spectroscopy and electron-spin resonance spectroscopy studies.

Keywords: chelates · copper · gels · halides · nanoparticles

[1] a) W. J. Rieter, K. M. Pott, K. M. L. Taylor, W. B. Lin, *J. Am. Chem. Soc.* **2008**, *130*, 11584–11585; b) I. Imaz, M. Rubio, L. García, F. García, D. Ruiz-Molina, J. Hernando, V. Puntes, D. Maspoch, *Chem. Commun.* **2010**, *46*, 4737–4739; c) G. Lu, J. T. Hupp, *J. Am. Chem. Soc.* **2010**, *132*, 7832–7833; d) H. Maeda, M. Hasegawa, T. Hashimoto, T. Kakimoto, S. Nishio, T. Nakanishi, *J. Am. Chem. Soc.* **2006**, *128*, 10024–10025; e) P. Horcajada, T. Chalati, C. Serre, B. Gillet, C. Sebrie, T. Baati, J. F. Eubank, D. Heurtaux, P. Clayette, C. Kreuz, J.-S. Chang, Y. K. Hwang, V. Marsaud, P.-N. Bories, L. Cynober, S. Gil, G. Férey, P. Couvreur, R. Gref, *Nat. Mater.* **2010**, *9*, 172–178; f) W. J. Rieter, K. M. L. Taylor, H. Y. An, W. L. Lin, W. Lin, *J. Am. Chem. Soc.* **2006**, *128*, 9024–9025; g) M. Oh, C. A. Mirkin, *Nature* **2005**, *438*, 651–654.

[2] a) S. K. Nune, P. K. Thallapally, A. Dohnalkova, C. Wang, J. Liu, G. J. Exarhos, *Chem. Commun.* **2010**, *46*, 4878–4880; b) X. Sun, S. Dong, E. Wang, *J. Am. Chem. Soc.* **2005**, *127*, 13102–13103; c) D. Tanaka, A. Henke, K. Albrecht, M. Moeller, K. Nakagawa, S. Kitagawa, J. Groll, *Nat. Chem.* **2010**, *2*, 410–416; d) W. Cho, H. J. Lee, M. Oh, *J. Am. Chem. Soc.* **2008**, *130*, 16943–16946; e) I. Imaz, J. Hernando, D. Ruiz-Molina, D. Maspoch, *Angew. Chem.* **2009**, *121*, 2361–2365;

Angew. Chem. Int. Ed. **2009**, *48*, 2325–2329; f) I. Imaz, D. Maspoch, C. Rodriguez-Blanco, J. M. Perez-Falcon, J. Campo, D. Ruiz-Molina, *Angew. Chem.* **2008**, *120*, 1883–1886; *Angew. Chem. Int. Ed.* **2008**, *47*, 1857–1860; g) D. M. Vriezema, J. Hoogboom, K. Velonia, K. Takazawa, P. C. M. Christianen, J. C. Maan, A. E. Rowan, R. J. M. Nolte, *Angew. Chem.* **2003**, *115*, 796–800; *Angew. Chem. Int. Ed.* **2003**, *42*, 772–776.

[3] To date, to the best of our knowledge, there is only one report of NMOPs supporting metallogelation: T. D. Hamilton, D.-K. Bučar, J. Baltrusaitis, D. R. Flanagan, Y. Li, S. Ghorai, A. V. Tivanski, L. R. MacGillivray, *J. Am. Chem. Soc.* **2011**, *133*, 3365–3371.

[4] a) K. H. Park, K. Jang, S. U. Son, D. A. Sweigart, *J. Am. Chem. Soc.* **2006**, *128*, 8740–8741; b) L. Catala, F. Volatron, D. Brinzel, T. Mallah, *Inorg. Chem.* **2009**, *48*, 3360–3370; c) E. Coronado, J. R. Galán-Mascaros, M. Monrabal-Capilla, J. García-Martinez, P. Pardo-Ibáñez, *Adv. Mater.* **2007**, *19*, 1359–1361; d) I. Boldog, A. B. Gaspar, V. Martínez, P. Pardo-Ibañez, V. Ksenofontov, A. Bhattacharjee, P. Gütlich, J. A. Real, *Angew. Chem.* **2008**, *120*, 6533–6537; *Angew. Chem. Int. Ed.* **2008**, *47*, 6433–6437; e) N. Kerbellec, L. Catala, C. Daiguebonne, A. Gloter, O. Stephan, J. C. Bunzli, O. Guillou, T. Mallah, *New J. Chem.* **2008**, *32*, 584–587; f) X. Zhang, Z. K. Chen, K. P. Loh, *J. Am. Chem. Soc.* **2009**, *131*, 7210–7211.

[5] a) J. H. Lee, H. Lee, S. Seo, J. Jaworski, M. L. Seo, S. Kang, J. Y. Lee, J. H. Jung, *New J. Chem.* **2011**, *35*, 1054–1059; b) J. H. Lee, S. Kang, J. Y. Lee, J. H. Jung, *Soft Matter* **2012**, *8*, 6557–6563.

[6] a) M-O. M. Piepenbrock, N. Clarke, J. W. Steed, *Soft Matter* **2010**, *6*, 3541–3547; b) M.-O. M. Piepenbrock, N. Clarke, J. W. Steed, *Langmuir* **2009**, *25*, 8451–8456; c) J. W. Steed, *Chem. Soc. Rev.* **2010**, *39*, 3686–3699; d) H. Lee, J. H. Lee, S. Kang, J. Y. Lee, G. John, J. H. Jung, *Chem. Commun.* **2011**, *47*, 2937–2939; e) S. Banerjee, N. N. Adarsh, P. Dastidar, *Soft Matter* **2012**, *8*, 7623–7629; f) S. Banerjee, D. P. Kumar, S. Bandyopadhay, N. N. Adarsh, P. Dastidar, *Cryst. Growth Des.* **2012**, *12*, 5546–5554.

[7] a) R. Aggarwal, V. Kumar, P. Tyagi, S. P. Singh, *Bioorg. Med. Chem.* **2006**, *14*, 1785–1791; b) V. Kumar, R. Aggarwal, P. Tyagi, S. P. Singh, *Eur. J. Med. Chem.* **2005**, *40*, 922–927; c) J. L. Kane, Jr., B. H. Hirth, B. Liang, B. B. Gourlie, S. Nahill, G. Barsomian, *Bioorg. Med. Chem. Lett.* **2003**, *13*, 4463–4466; d) O. Prakash, R. Kumar, V. Parkash, *Eur. J. Med. Chem.* **2008**, *43*, 435–440; e) O. Prakash, D. K. Aneja, P. Lohan, K. Hussain, S. Arora, C. Sharma, K. R. Aneja, *Med. Chem. Res.* **2012**, *21*, 2961–2968.

[8] C. M. Pask, K. D. Camm, C. A. Kilner, M. A. Halcrow, *Tetrahedron Lett.* **2006**, *47*, 2531–2534.

Received: November 28, 2012